Substructure in Galaxy Clusters Identified by Double-Lobed Radio Sources

Joshua Wing & Elizabeth Blanton (Boston University)

ABSTRACT

Using radio sources from the FIRST survey, and optical counterparts in the SDSS, we have identified a large number of galaxy clusters. These radio sources are driven by AGN, and our cluster sample includes objects with bent, and straight, double-lobed sources. We also included a single-component comparison sample. We examine these galaxy clusters for evidence of optical substructure, testing the possibility that bent sources are formed in large-scale mergers. We use a suite of substructure analysis tools to determine the location and extent of substructure visible in the optical distribution of cluster galaxies. We also examine the X-ray structure of sources with available Chandra observations for additional evidence of substructure and as a comparison to our optical tests.

INTRODUCTION

Galaxy clusters are excellent laboratories for studying galaxy formation and evolution. Identifying double-lobed radio sources and the optical source they are associated with can lead to the discovery of a significant number of previously unknown galaxy clusters. A substantial fraction of bent double-lobed radio sources that lack optical IDs in the SDSS are likely to be associated with galaxy clusters at high redshifts (z>0.8). Using these sources will provide a systematic way of searching for high-z galaxy clusters.

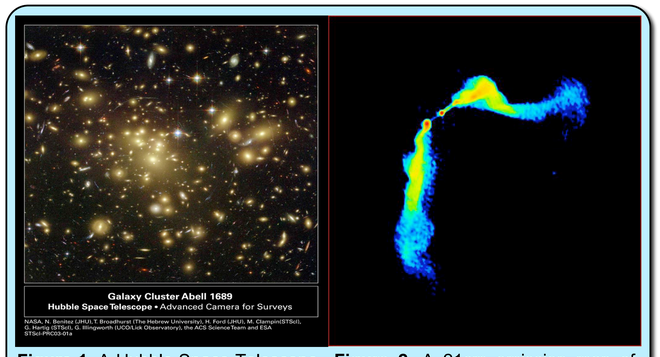

Figure 1. A Hubble Space Telescope image of the galaxy cluster Abell 1689.

Figure 2. A 21cm emission map of 3C465. The morphology seen is typical of the bent double-lobed sources we examined.

DEFINING THE SAMPLES

Wing & Blanton (2011) used visually selected bent-lobed FIRST sources from Blanton et al. (2000) and automatically selected bent- and straight-lobed sources selected using a decision tree algorithm program from Proctor (2006). We also defined a sample of randomly selected single-component radio sources (a FIRST source having no other radio source within 60") as a comparison between double-lobed sources and much more typical single-component sources. The number of sources in each sample is shown in Table 1. We are investigating the effect that the cluster environment has on the bending of radio lobes, as well as establishing that these bent-lobed radio sources (which can be observed in the FIRST catalog up to z~2) are efficient signposts for locating high-redshift galaxy clusters.

Sample	Total	SDSS 95%	Color Cut	FR I	FR II
Visual-Bent	384	272	166	109	57
Auto-Bent	1,546	599	272	171	101
Straight	3,232	1,288	449	263	186
1 Comp	3,348	782	358	335	23

Table 1. Total number of sources in each sample after our selections, with the color cut representing the selection of red elliptical galaxies shown in Figure 3.

IDENTIFYING ASSOCIATED SOURCES

Wing & Blanton (2011) searched SDSS for optical sources within 5" of the radio source's central component. Using the closest optical source, we determined a 95% reliability separation cut-off for each sample compared to a sample of random positions on the sky. Radio source ids that have blue colors and high-z (likely quasars) were removed from the samples. We measured cluster richness by searching SDSS for sources within a radius of 1 Mpc around each radio/optical source and brighter than M_r=-18. Background galaxy counts were subtracted and a richness was calculated. A count above 40 corresponds to a cluster.

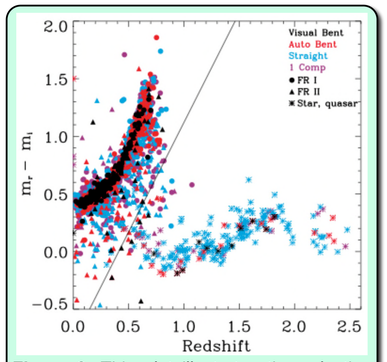

Figure 3. This plot illustrates the selection we made for red elliptical galaxies. The sources lying below and to the right of the line are most likely quasars and are removed from cluster consideration in the current work.

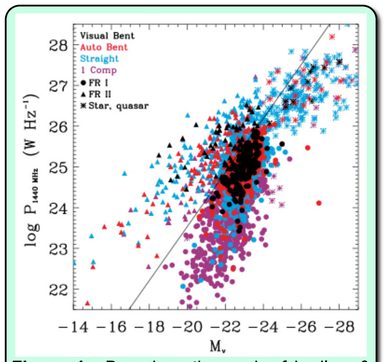

Figure 4. Based on the work of Ledlow & Owen (1996), we were able to classify radio sources as FR I/II based on radio power and M_r. FR II sources are generally more powerful and luminous. We also visually classified every radio source as FR I/II.

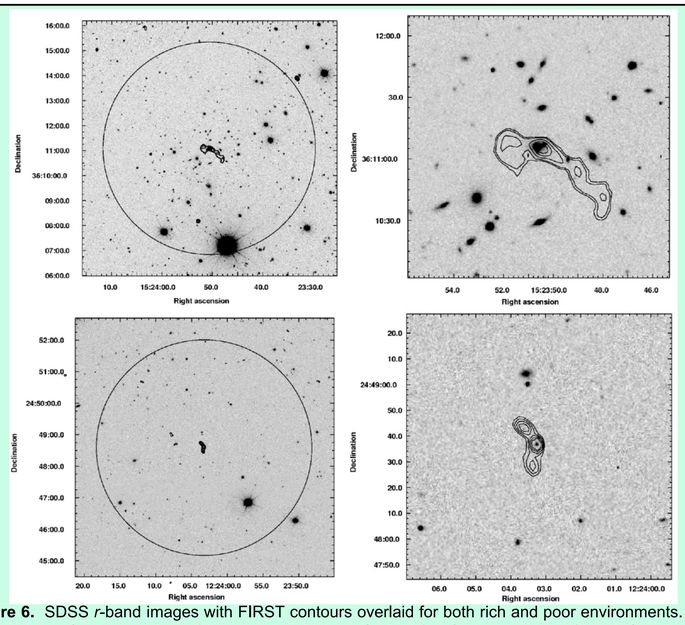

Figure 6. SDSS *r*-band images with FIRST contours overlaid for both rich and poor environments. The left-hand panels show a view of the area in which we looked for cluster members (the circles show an area with a radius of 1.0 Mpc around the radio source), the right-hand panels show a zoomed-in (250x250 kpc) view. The top panels show a rich cluster located at a redshift of z=0.25 and richness of 102. The bottom panels show a non-cluster located at a redshift of z=0.32 and richness of -9.

SUBSTRUCTURE TESTS

The first test is the Δ test, finding the local average velocity and standard deviation for each galaxy in the cluster. The difference between these values compared to global values are calculated for each galaxy. The sum of these values becomes Δ. The next test was the ε test. This test measures the local mass around each galaxy in the cluster. The overall statistic is the average local mass around each galaxy. Clusters with substructure will have lower ε values. The last test is the α (centroid shift) test. The center of the cluster in x and y coordinates is found and compared to the center calculated using weights based on the local velocity dispersion of each galaxy. Thus, α is the average of the difference in un-weighted and weighted centers. Each test was normalized using 500 Monte Carlo simulations with randomized velocities.

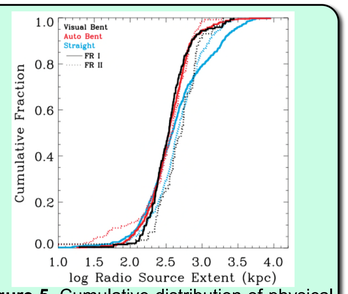

Figure 5. Cumulative distribution of physical extent of FR I and II sources. In general, FR II sources are larger than FR I sources.

Sample	Total	FR I	FR II
Visual-Bent	62%(98)	65%(85)	46%(13)
Auto-Bent	41%(120)	47%(97)	13%(23)
Straight	24%(217)	28%(164)	9%(53)
1 Comp	10%(209)	10%(202)	0%(7)

Table 2. Percentage of sources in each sample (total number in parenthesis) found in rich clusters. The second column is the overall fraction and the third and fourth columns are for FR I and II sources. We found that bent-lobed sources are more likely to be found in rich clusters, and FR I sources more likely than FR II sources.

DETERMINING OPTICAL SUBSTRUCTURE

We searched SDSS for sources with spectroscopicaly measured redshifts within a radius of 3 Mpc around each radio/optical source in our samples. We determined the average redshift of all galaxies in this area and within ±10000 km s^{-1} of the radio source after iteratively excluding all galaxies with peculiar velocity gaps of more than 1000 km s^{-1}. We used the shifting gapper method of Owers et al. (2009) to determine cluster members for potential clusters with more than 40 spectroscopically measured members in this velocity range. Using these cluster members we ran several substructure tests, as described in Pinkney et al. (1996) and below. The results described here are from three different 3D tests, each of which have their own strengths and weaknesses.

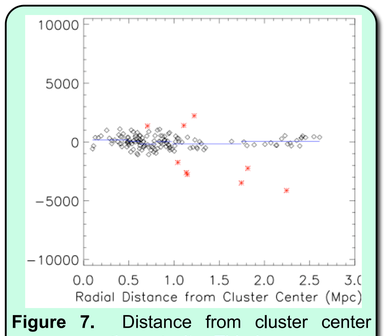

Figure 7. Distance from cluster center versus peculiar velocity. This is an example of the shifting gapper method. Sources not meeting the criteria are marked as red stars.

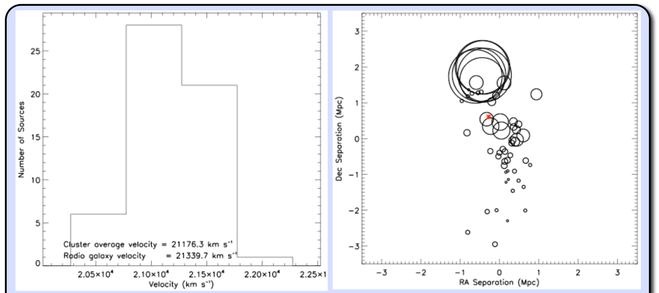

Figure 8. Velocity histogram (left) and a Dressler-Schectman bubble-plot for the source J105147.5+552309. The velocity histogram shows a clear peak at a slightly lower (~200 km s^{-1}) recessional velocity than that of the radio galaxy. The bubble-plot shows the ∂ values for each of the cluster members. A larger radius circle implies the presence of substructure. This is a cluster with significant substructure according to the Dressler-Schectman statistic (Δ=1.32). The red star shows the location of the radio galaxy.

RESULTS

One possible explanation for bent-lobed radio sources is that a cluster-cluster merger imparts bulk motion to the ICM, and the radio lobes are bent by ram pressure. A large amount of substructure is a good indicator of a recent cluster-cluster merger. If this causes radio lobe bending, we would expect to see more substructure in bent-lobed sources. Based on current analysis, we see no correlation between substructure and the bending of lobes.

Sample	Number	Delta	Epsilon	Alpha
Visual-Bent	7	71%	71%	43%
Auto-Bent	10	60%	50%	60%
Straight	6	100%	50%	67%
1 Comp	5	80%	60%	60%

Table 3. Percentage of sources in each sample that have significant substructure. We find similar rates of substructure in clusters associated with all of our different radio samples. The number of sources (column 2) is less than that in Table 1 because of our requirement that each cluster have a minimum of 40 spectroscopicaly measured redshifts within the area and velocity range mentioned previously. Sources have significant substructure if less than 10% of the 500 randomized Monte Carlo simulations have more substructure than the actual cluster.

CURRENT WORK

Follow-up observations of bent-lobed sources could likely be an efficient way of locating distant clusters of galaxies. We are currently observing many of our high-z candidates in the optical and NIR. Future X-ray observations of these high-z clusters will help in constraining cosmological parameters, including the equation of state of dark energy as in Allen et al. (2004).

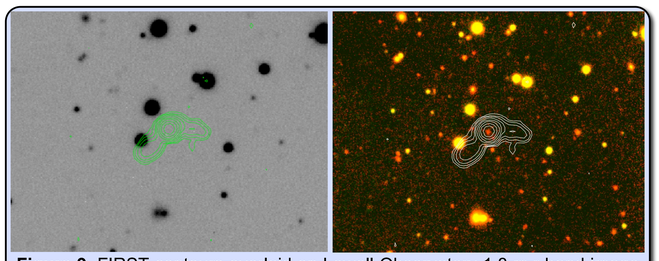

Figure 9. FIRST contours overlaid on Lowell Observatory 1.8 m r-band image (left) as well as recent Mayall 4 m NEWFIRM combined J- and K-band images (right) of the radio source J073406+293316. This source has no optical counterpart down to the limit of reliability in the r-band (r~23), but with deeper NIR observations we clearly see that there is a galaxy associated with this radio source. The host galaxy and numerous associated galaxies are detected in the combined JK image at z > 0.8. Red objects are distant galaxies and yellow objects are stars or nearby galaxies.

BIBLIOGRAPHY

Allen, S. W., Schmidt, R. W., Ebeling, H., Fabian, A. C., & van Speybroeck, L. 2004, MNRAS, 353, 457
Blanton, E.L., Gregg, M.D., Helfand, D.J., Becker, R.H., & White, R.L. 2000, ApJ, 531, 118
Ledlow, M.J. & Owen, F.N. 1996, AJ, 112, 9
Owers, M.S., Nulsen, P.E.J., Couch, W.J., Markevitch, M., & Poole, G.B. 2009, ApJ, 692, 702
Pinkney, J., Roettiger, K., & Burns, J.O. 1996, ApJS, 104, 1
Proctor, D.D. 2006, ApJS, 165, 95P
Wing, J.D. & Blanton, E.L. 2011, AJ, 141, 88